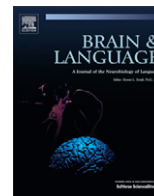


Contents lists available at [SciVerse ScienceDirect](http://www.sciencedirect.com)

Brain & Language

journal homepage: www.elsevier.com/locate/b&l

Anatomy of the visual word form area: Adjacent cortical circuits and long-range white matter connections

Jason D. Yeatman^{a,*}, Andreas M. Rauschecker^{a,b,*}, Brian A. Wandell^{a,c}

^a Psychology Department, Stanford University, Stanford, CA 94305, United States

^b Neurosciences Program and Medical Scientist Training Program, United States

^c Stanford Center for Cognitive and Neurobiological Imaging, United States

ARTICLE INFO

Article history:

Available online xxx

Keywords:

Visual word form area (VWFA)
Diffusion tensor imaging (DTI)
Retinotopy
Vertical occipital fasciculus
Sagittal stratum
Inferior frontal occipital fasciculus (IFOF)
Inferior longitudinal fasciculus (ILF)

ABSTRACT

Circuitry in ventral occipital-temporal cortex is essential for seeing words. We analyze the circuitry within a specific ventral–occipital region, the visual word form area (VWFA). The VWFA is immediately adjacent to the retinotopically organized VO-1 and VO-2 visual field maps and lies medial and inferior to visual field maps within motion selective human cortex. Three distinct white matter fascicles pass within close proximity to the VWFA: (1) the inferior longitudinal fasciculus, (2) the inferior frontal occipital fasciculus, and (3) the vertical occipital fasciculus. The vertical occipital fasciculus terminates in or adjacent to the functionally defined VWFA voxels in every individual. The vertical occipital fasciculus projects dorsally to language and reading related cortex. The combination of functional responses from cortex and anatomical measures in the white matter provides an overview of how the written word is encoded and communicated along the ventral occipital-temporal circuitry for seeing words.

© 2012 Elsevier Inc. All rights reserved.

1. Introduction

In their studies of reading disorders in neurological patients, Warrington and colleagues found support for the existence of a visual word-form system “which parses (multiply and in parallel) letter strings into ordered familiar units and categorizes these units visually (p. 110)”. The methods of neurology available to Warrington and colleagues yielded inconsistent evidence about the location of this system. They speculated that the anatomical locus of acquired dyslexia might be in ventral occipital temporal cortex (Kinsbourne & Warrington, 1963) or in temporal parietal cortex (Warrington & Shallice, 1980).

During the following decades, advances in neuroimaging measurements provided compelling evidence that regions within ventral occipital-temporal (VOT) cortex are part of the network for skilled reading (Dehaene, Le Clec, Poline, Le Bihan, & Cohen, 2002; Nobre, Allison, & McCarthy, 1994; Petersen, Fox, Snyder, & Raichle, 1990; Price et al., 1994; Salmelin, Helenius, & Service, 2000; Salmelin, Service, Kiesila, Uutela, & Salonen, 1996; Wandell, 2011; Wandell, Rauschecker, & Yeatman, 2012). Damage in this region or nearby white matter can result in selective reading deficits (Cohen et al., 2003; Damasio & Damasio, 1983; Epelbaum et al.,

2008; Gaillard et al., 2006; Greenblatt, 1973); VOT responses are relatively weak in poor readers (Maisog, Einbinder, Flowers, Turkeltaub, & Eden, 2008); in healthy skilled readers, VOT circuitry is highly responsive to visual word forms (Ben-Shachar, Dougherty, Deutsch, & Wandell, 2007b; Dehaene et al., 2002, 2011; McCandliss, Cohen, & Dehaene, 2003); during development, improvements in reading performance are correlated with increases in VOT responses to written words (Ben-Shachar, Dougherty, Deutsch, & Wandell, 2011; Brem et al., 2010; Maurer, Brem, Bucher, & Brandeis, 2005). Cohen and colleagues proposed that within the extensive cortical region of VOT there is a specific location – the visual word form area (VWFA) – that is the key neuronal circuitry that learns to recognize word forms (Cohen et al., 2002). The specific functional role of the VWFA within the word-form system is debated (Dehaene & Cohen, (2011); Price & Devlin, 2003, 2011; Vogel, Miezin, Petersen, & Schlaggar, 2011).

Skilled reading must involve multiple brain regions. Thus, Warrington’s observations that damage in either VOT or temporal parietal cortex may impair reading are still relevant. For example, Greenblatt (1973) reported that damage to the vertical occipital fasciculus, a fiber tract that connects ventral occipital with dorsal–lateral occipital regions, results in pure alexia, also called alexia without agraphia or word blindness. Thus damage affecting either cortical region, or the circuitry carrying signals between them, may result in letter-by-letter reading.

There is no definitive demonstration of a cortical circuit that performs a single cognitive function. It is particularly unlikely that a region dedicated uniquely to reading exists; after all, reading has

* Corresponding authors. Address: Wandell Laboratory, Jordan Hall, Building 420, Stanford University, Stanford, CA 94305, United States.

E-mail addresses: jyeatman@stanford.edu (J.D. Yeatman), andreas@stanford.edu (A.M. Rauschecker).

¹ These authors contributed equally to this work.

only become important to society over the last few hundred years. To understand the VWFA function, and how this might contribute to reading, we can rely on two general cortical principles. First, cortical circuits with similar functions are often clustered together (Brewer, Liu, Wade, & Wandell, 2005; Wandell, Dumoulin, & Brewer, 2007); such clustered regions are typically connected by the U-fibers system within the white matter. To understand the VWFA's role in reading we should consider the properties of adjacent cortical circuitry. Second, cortical circuits communicate with specific and targeted distant cortical regions via long-range axon bundles. To further understand the role of the VWFA's role in reading, it will be helpful to delineate its long-range connections.

Improvements in the resolution and signal quality of functional and structural magnetic resonance imaging (MRI) have made it possible to map reliably the VWFA and nearby cortical circuitry in single subjects using functional MRI (fMRI), and to estimate long-range inputs and outputs using diffusion weighted imaging (DWI). The fMRI measurements situate the VOT circuitry involved in seeing words with respect to other important cortical regions; the diffusion measurements provide insight into the long-range connections between VOT and other cortical regions. Recent reviews have emphasized the importance of a circuit diagram for reading, and specifying the inputs and outputs of the VWFA (Price & Devlin, 2011; Wandell et al., 2012). Here, we describe new measurements of these properties in the brains of individual subjects.

2. Methods and materials

The subjects and data used in this study have been described in previous reports from our group (Ben-Shachar, Dougherty, Deutsch, & Wandell, 2007a; Rauschecker et al., 2011; Yeatman et al., 2011).

2.1. fMRI data acquisition

2.1.1. Scanning parameters

Anatomical and functional imaging data were acquired on a 3 T General Electric scanner using an 8-channel head coil. Head motion was minimized by placing padding around the head. Functional MR data were acquired using a spiral pulse sequence (Glover, 1999). Thirty 2.5 mm thick coronal oblique slices oriented approximately perpendicular to the calcarine sulcus were prescribed. These slices covered the whole occipital lobe and parts of the temporal and parietal lobes. Data were acquired using the following parameters: Acquisition matrix size = 64×64 , FOV = 180 mm, voxel size of $2.8 \times 2.8 \times 2.5$ mm, TR = 2000 ms, TE = 30 ms, flip angle = 77° . Some retinotopy scans were acquired with 24 similarly oriented slices at a different resolution ($1.25 \times 1.25 \times 2$ mm, TR = 2000 ms, TE = 30 ms). Stimuli were projected onto a screen that the subject viewed through a mirror fixed above the head. The screen subtended a radius of 12° along the vertical dimension.

2.1.2. Experimental design

The visual word form area (VWFA) localizer consisted of four block-design runs of 180 s each. Twelve-second blocks of words, fully phase-scrambled words, or checkerboards alternated with 12-s blocks of fixation (gray screen with fixation dot). Stimuli during each block were shown for 400 ms, with 100 ms inter-stimulus intervals, giving 24 unique stimuli per block. Words were six-letter nouns with a minimum word frequency of seven per million. The size of all stimuli was $14.2 \times 4.3^\circ$. Fully phase-scrambled words consisted of the same stimuli, except that the phase of the images was randomized. Checkerboard stimuli reversed contrast at the same rate as the stimuli changed and were the same size as other stimuli. The order of the blocks was pseudo-randomized, and the

order of stimuli within those blocks was newly randomized for each subject.

2.2. fMRI data analysis

fMRI data were analyzed using the freely available mrVista tools (<http://white.stanford.edu/software/>, SVN revision 2458). We used an affine transformation to align each temporal volume to the first volume of the first run. Baseline drifts were removed from the time series by high-pass temporal filtering (cut-off frequency: 20 frames per scan). A general linear model (GLM) was fit to each voxel's time course, estimating the relative contribution of each condition to the time course. We also included a separate regressor for each run to account for shifts in baseline. Statistical maps were computed as voxel-wise *t*-tests between two conditions. For visualization, statistical contrast maps were interpolated to the T1-weighted volume anatomy and restricted to gray matter layers. These maps were projected onto a cortical surface rendering consisting of the surface along the gray–white boundary. Spatial smoothing was applied only for visualization on the 3-D rendering and not for data analyses.

We combined retinotopic mapping and a VWFA localizer using standard statistical contrasts (Fig. 1). The statistical processing is described in detail by Rauschecker et al. (2011). The VWFA was defined in individuals by contrasting words to phase scrambled words, presented at the fovea. The VWFA localizer statistical contrast produces clusters of significant voxels within VOT cortex in all subjects. For all subjects, we find that the location of the VWFA is just lateral and/or anterior to the visual field maps VO-1 and VO-2 (Brewer et al., 2005). The TO-1 and TO-2 visual field maps (Amano, Wandell, & Dumoulin, 2009) are part of the human motion-selective complex (hMT+) that is generally located superior and lateral to the VWFA; however, in some subjects the VWFA abuts these maps. In ten of eleven subjects words presented at fixation produce activation at homologous locations the left (VWFA) and right hemispheres. We refer to the right hemisphere location as the rVWFA.

The VWFA was defined in each subject as ventral surface activation from a contrast between words and phase-scrambled words ($p < 0.001$, uncorrected). The region was restricted to responsive voxels outside retinotopic areas and anterior to hV4. The Montreal Neurological Institute (MNI) coordinates of the peak voxel within the ROI was identified by finding the best-fitting transform between the individual T1-weighted anatomy with the average MNI T1-weighted anatomy and then applying that transform to the peak voxel within the VWFA for the same contrast.

The VWFA ROIs are located near the left lateral occipito-temporal sulcus and within ~ 5 mm of previous reports (Ben-Shachar et al., 2007b; Cohen et al., 2002; Dehaene et al., 2002). In this manuscript, unless otherwise specified, VWFA refers to the left-hemisphere ROI. In all subjects a contrast of words versus checkerboards produces regions of interest in virtually identical locations and of similar size.

We identified retinotopic areas in each individual using the previously described population receptive field method (Dumoulin & Wandell, 2008). Briefly, this method finds the best fitting 2-D Gaussian receptive field, consisting of an x, y visual field position and σ , the receptive field size, for each voxel in response to bars of flashing checkerboards sweeping across the visual field. Retinotopic areas were defined by angle reversals (Wandell & Winawer, 2010; Wandell et al., 2007).

2.3. Diffusion data acquisition

Diffusion data were acquired on a 1.5 T Signa LX scanner (Signa CVi; GE Medical Systems, Milwaukee, WI) using a self-shielded,

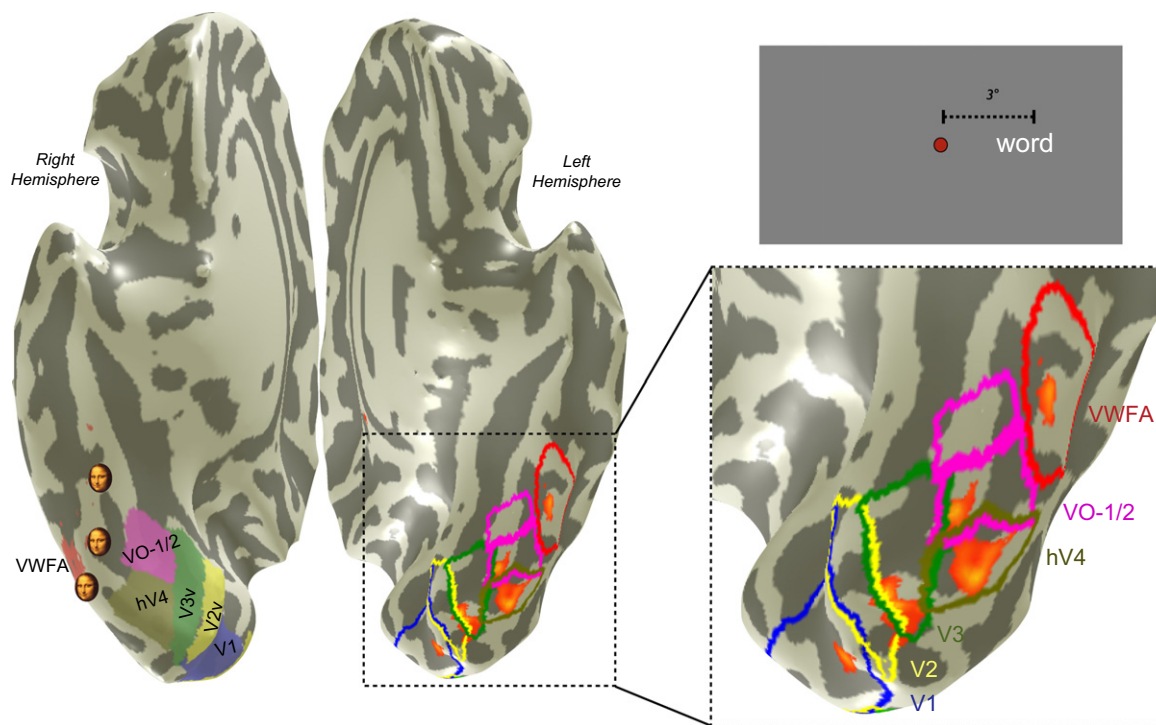


Fig. 1. The location of the VWFA in relation to visual field maps. The image at the left is a ventral view of the cortex in a single subject. The cortex is inflated; the shading indicates the positions of gyri (light) and sulci (dark). Visual field maps [V1, V2, V3, hV4, VO-1, VO-2] were defined by retinotopic mapping, and the VWFA was defined by a standard localizer. The ventral maps, VWFA and right VWFA (rVWFA) are shown as colored regions on the right hemisphere and colored borders on the left hemisphere. Small faces indicate face-selective regions of interest (mFus, pFus, IOG, right hemisphere) based on the mean Talarach coordinates of activations in 11 subjects. The overlaid orange–red heatmap on the left hemisphere are significant fMRI responses ($p < 10^{-4}$) to a word positioned 3° to the right of fixation (see inset at upper right), contrasted with a word 3° to the left of fixation. Significant activations occur within several visual maps and the VWFA. The activations are at positions that are expected based on the location of the word in the visual field. For simplicity, only the largest cluster of the VWFA region of interest is shown in the left hemisphere.

high-performance gradient system. A standard quadrature head coil, provided by the vendor, was used for excitation and signal reception.

The diffusion protocol used eight repetitions of a 90-s whole-brain scan. The scans were averaged to improve signal quality. The pulse sequence was a diffusion-weighted single-shot spin-echo, echo planar imaging sequence (63 ms TE; 6 s TR; 260 mm FOV; 128×128 matrix size; ± 110 kHz bandwidth; partial k-space acquisition). We acquired 60 axial, 2-mm-thick slices (no skip) for two b -values, $b = 0$ and $b = 800$ s/mm². The high b -value data were obtained by applying gradients in 12 diffusion directions (six non-collinear directions). Two gradient axes were energized simultaneously to minimize TE and the polarity of the effective diffusion-weighting gradients was reversed for odd repetitions to reduce cross-terms between diffusion gradients and imaging and background gradients.

We also acquired and analyzed a 40-diffusion direction sequence for a subset of the subjects. By comparing the fiber tract estimates from the two independent datasets we confirmed that the trajectory and endpoints of fascicles we report here were not influenced the specific acquisition parameters. Consistent with our previous reports the principal diffusion direction estimates (and scalar estimates of fractional anisotropy, mean diffusivity, radial diffusivity and axial diffusivity) were very similar for the 12 diffusion direction and 40 diffusion direction acquisitions (Yeatman et al., 2011). For all the analyses in this paper, including tractography, there were no differences between estimates using 12- and 40-directions because the data were acquired at relatively low b -values that only support fitting a tensor model as oppose to more a more complex model.

We collected T1-weighted anatomical images for each subject using an 8-min sagittal 3D-SPGR sequence (1-mm isotropic vox-

els). The following anatomical landmarks were defined manually in the T1 images: the anterior commissure (AC), the posterior commissure (PC), and the mid-sagittal plane. With these landmarks, we used a rigid-body transform to convert the T1-weighted images to the conventional AC–PC aligned space.

2.4. Diffusion data processing

Eddy current distortions and subject motion in the diffusion-weighted images were removed by a 14-parameter constrained non-linear co-registration based on the expected pattern of eddy-current distortions given the phase-encode direction of the acquired data (Rohde, Barnett, Basser, Marengo, & Pierpaoli, 2004).

Each diffusion-weighted image was registered to the mean of the (motion-corrected) non-diffusion-weighted ($b = 0$) images using a two-stage coarse-to-fine approach that maximized the normalized mutual information. The mean of the non-diffusion-weighted images was automatically aligned to the T1 image using a rigid body mutual information algorithm. All raw images from the diffusion sequence were resampled to 2-mm isotropic voxels by combining the motion correction, eddy-current correction, and anatomical alignment transforms into one omnibus transform and resampling the data using a trilinear interpolation algorithm based on code from SPM5 (Friston & Ashburner, 2004). An eddy-current intensity correction (Rohde et al., 2004) was applied to the diffusion-weighted images at the resampling stage.

The rotation component of the omnibus coordinate transform was applied to the diffusion-weighting gradient directions to preserve their orientation with respect to the resampled diffusion images.

2.5. Tractography

Fiber tracts were estimated using a deterministic streamlines tracking algorithm (STT) (Basser, Pajevic, Pierpaoli, Duda, & Aldroubi, 2000; Mori, Crain, Chacko, & Van Zijl, 1999) with a fourth-order Runge–Kutta path integration method and 1-mm fixed-step size. Tensors were fit to each diffusion data sample point using a robust least-squares algorithm designed to remove outliers from the tensor estimation step (Chang, Jones, & Pierpaoli, 2005). A continuous tensor field was estimated with trilinear interpolation of the tensor elements. Starting from initial seed points within the white matter mask, the path integration procedure traced streamlines in both directions along the principal diffusion axes. Individual streamline integration was terminated using two standard criteria: tracking is halted if (a) the FA estimated at the current position is below 0.15, or (b) the minimum angle between the last path segment and next step direction is $>50^\circ$.

All custom image processing software is available as part of our open-source mrDiffusion package available for download from (<http://white.stanford.edu/software/>, SVN revision 2458).

3. Results

3.1. Visual field maps and the VWFA

Responses in V1 and nearby cortical regions (V2, V3, hV4, VO-1, VO-2) are organized into retinotopic maps (Wandell & Winawer, 2010; Wandell et al., 2007). Viewing a single word evokes a series of responses in several of these maps (Fig. 1). A word evokes a response in primary visual cortex (V1) at a position that corresponds

to the word's visual field position; for example, a word positioned on the horizontal meridian, just to the right of fixation, elicits a response in the depth of calcarine sulcus (V1). There are also responses at the boundary between V2 and V3, which is the horizontal meridian representation of those maps, and within the hV4 and VO-1 maps. Text also elicits a response within the VWFA, a region that can be identified in a separate localizer scan that compares the responses to words and phase-scrambled words. These regions all respond to many types of spatial patterns (e.g. checkerboards or gratings); none respond uniquely to words.

The relative positions of the visual field maps and the responses to a word are consistent across subjects (Fig. 2A). The reliability of the spatial relationships between the maps provides a very useful coordinate frame for identifying the same activation in different subjects. The absolute position and size of the visual field maps, however, can differ between subjects. The surface area of the V1 map, for example, differs by more than a factor of two and the surface area does not correlate with brain size (Andrews, Halpern, & Purves, 1997; Dougherty et al., 2003). Moreover, given the relatively small size of the word in the visual field, there is a correspondingly small surface area responding in the V1–V3 maps. Given the variability in map size and brain convolutions, averaging responses from multiple subjects in an atlas reference frame is likely to conflate responses between visual field maps, face-selective and object-selective cortex, and the VWFA. To monitor activations at a few millimeters of spatial resolution, we measure single subjects.

The region identified as VWFA in these two subjects consists of several small clusters of voxels anterior to hV4 and outside of the VO-1 and VO-2 maps. The MNI coordinates of these activations are consistent with the VWFA description in the literature, and both

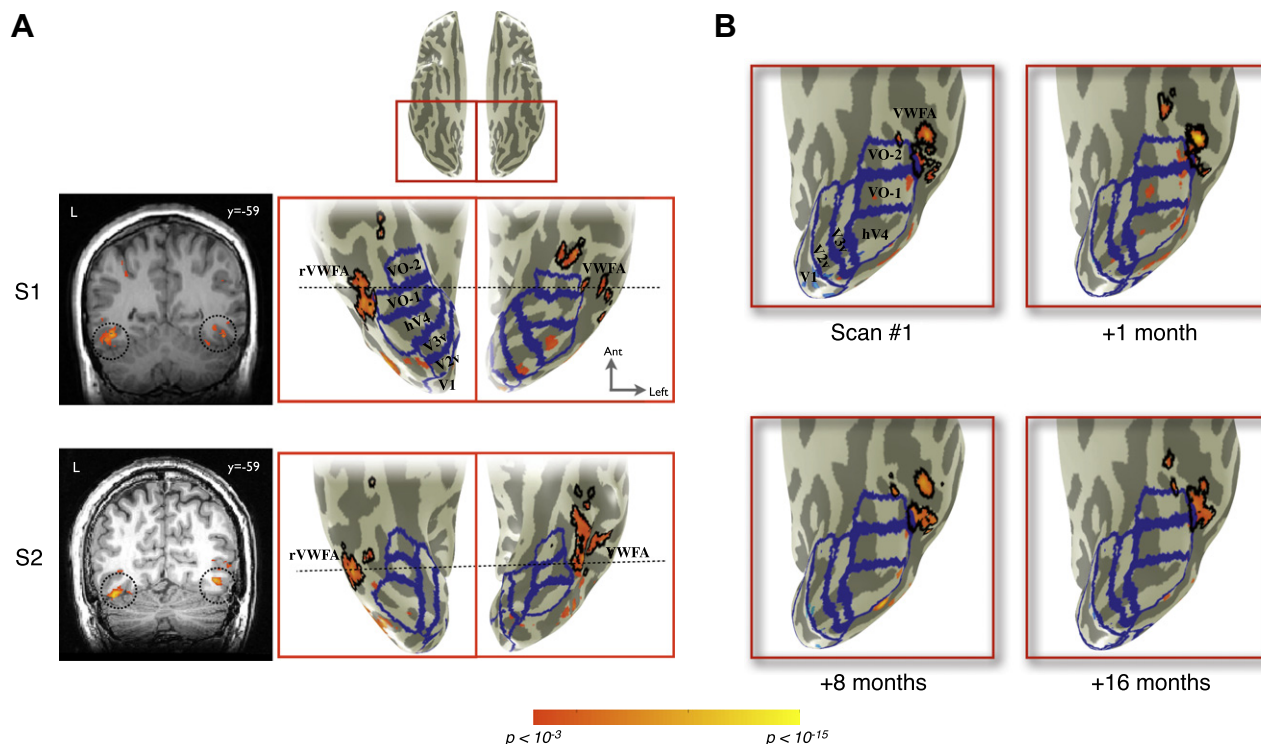


Fig. 2. Inter-subject differences and within-subject stability of VWFA localization. (A) The VWFA localizer (words $>$ phase-scrambled words, $p < 10^{-3}$) produces areas of significant activation in VOT cortex in left and right hemispheres. The activations are shown for two typical subjects on a single coronal slice (left) and on an inflated cortical surface (right). Blue outlines indicate the boundaries of visual field maps. The black outlines indicate the boundaries of the VWFA and rVWFA regions of interest as defined in the main text. Dotted horizontal lines indicate approximate locations of coronal slices. The MNI y-coordinate (anterior–posterior axis) is indicated next to the coronal slices. VOT cortex is shown from a ventral view (left hemisphere is on right side). Inset at top indicates the magnified region of this ventral view of VOT cortex. (B) The VWFA localizer was repeated four times in the same individual (last scan 16 months after first scan). The VWFA (black boundaries) was defined as significant ($p < 10^{-3}$) activity outside visual field maps (blue boundaries). Only the left hemisphere is shown for simplicity. The measured location of the VWFA is stable over time.

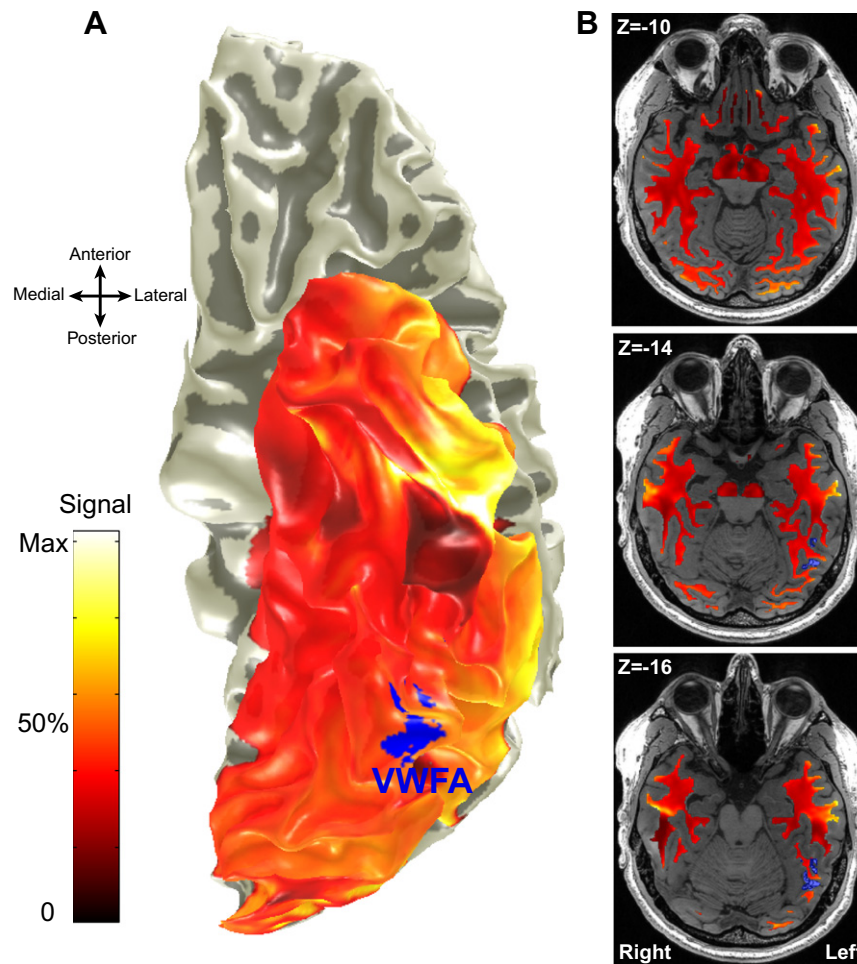


Fig. 3. Mean diffusion weighted imaging signal intensity in the ventral occipital and temporal lobes. (A) Cortical Surface rendering showing the mean signal intensity measured in the cortex with a spin-echo DWI sequence. T2* weighted gradient-echo measurements of the temporal lobe show substantial signal loss immediately anterior to the VWFA, however spin-echo measurements do not. (B) Axial slices through the white matter adjacent to the VWFA showing the mean DWI signal intensity. There is not signal loss in the white matter. Imaging artifacts are unlikely to substantially impact fiber tractography in the white matter near the VWFA.

regions respond to the word versus checkerboard contrast. Yet, the precise organization of these response patches differs. The patchy pattern may reflect underlying clusters of neurons sensitive to word-like stimuli. Processing systems organized into a distributed set of cortical patches is currently under active investigation for face perception (Weiner & Grill-Spector, 2010), and this may be a general architecture for cortical specializations.

Alternatively, the VWFA patches may be due to uneven sensitivity of the fMRI measurement. An important limitation in ventral occipital measurements concerns an artifact created by transverse dural venous sinus (Winawer, Horiguchi, Sayres, Amano, & Wandell, 2010). The sinus distorts the local magnetic field and masks certain cortical responses. Consequently, responses that are easy to measure in one subject may be present but hidden by the local imaging artifacts in another. The VWFA response is located near this sinus in some subjects, and we suspect that some of the between-subject variability in the response measured with gradient-echo BOLD imaging can be attributed to this artifact.

Within-subject measurements are relatively stable across time (Fig. 2B). For example, we measured one subject's VWFA in four separate scan sessions (1, 8, and 16 months following the first scan). The location of the VWFA just lateral to VO-2, with a smaller activation anterior to VO-2, is consistent across these four sessions. The localizer also consistently elicits significant activation in a location just lateral to hV4. The relatively small differences between measurements can be attributed to scanner noise. In sum-

mary, the spatial activity pattern in each subject is stable, and the relative position of the VWFA with respect to the maps is consistent. But the spatial distribution of measured VWFA patches differs between subjects.

3.2. White matter connections and the VWFA

The region of cortex near the VWFA has several deep sulci; consequently, the nearby white matter includes a number of narrow tendrils (Fig. 3). Determining the precise location on a gyrus where white matter fascicles terminate is not always possible because the thickness of white matter can be below the spatial resolution of the diffusion imaging data (~2 mm). Hence, as a tract approaches its cortical target, there is significant uncertainty in fiber orientation estimates.

The white matter projections to sulci, such as the lateral occipital-temporal sulcus (OTS), are more amenable to analysis. This region is likely to include white matter pathways from an array of cortical regions; some of these pathways must carry signals essential for reading. BOLD measurements in the temporal lobe, immediately anterior to the VWFA, are effected by magnetic susceptibility artifacts that cause substantial signal dropout in a typical gradient echo, T2* weighted imaging sequence (Wandell et al., 2012; Winawer et al., 2010). This artifact limits the ability to detect reading related signals because gradient echo pulse sequences are blind to activation in key regions of the anterior tem-

poral lobe. Magnetic susceptibility artifacts in the temporal lobe have less impact on spin echo pulse sequences used in diffusion imaging. The surface rendering in Fig. 3A shows the mean signal intensity measured in the cortex with a spin-echo DWI sequence. The axial images in Fig. 3B show the mean signal intensity in the white matter near the VWFA. There is little signal loss in the immediate vicinity of the VWFA, however there is signal loss in regions of cortex 2–3 cm anterior to the VWFA; this loss does not extend deeply into the white matter. Hence it is unlikely that imaging artifacts affect the identification of major white matter fascicles projecting to the VWFA; however cortical endpoints in the anterior temporal lobe may be masked by signal loss in cortex.

To identify major white matter fascicles that consistently pass within close proximity to the VWFA, we performed whole-brain streamlines tractography (STT) for each of 27 subjects. We then identified the streamlines that passed through a 7-mm radius sphere constructed around every subject's functionally defined VWFA. This region included the white matter near the OTS. The VWFA was defined as those cortical voxels that respond to written words significantly more than to phase-scrambled words ($p < 0.001$). The streamlines are estimates of fascicular bundles comprising thousands axons, some of which likely synapse on originate from neurons in the VWFA.

To summarize these peri-VWFA fascicles across subjects, we transformed the estimated tracts from different individuals into a common atlas space. Each voxel in this atlas space contains a tract from some number of subjects (between 0 and 27), and we represent this number by a color map (Fig. 4). The fascicular network near the VWFA contains projections capable of communicating efficiently with specific regions within the anterior temporal lobe, frontal lobe, and lateral occipital–parietal cortex.

The tract endpoints were consistent across subjects. The occipital lobe endpoints were concentrated in the inferior and middle occipital gyrus (BA 19), fusiform gyrus (BA 37), lingual and superior occipital gyrus (BA 18). Parietal lobe endpoints were concentrated in the angular gyrus, (BA 40). Frontal lobe endpoints were concentrated in the inferior frontal gyrus pars triangularis and pars orbitalis (BA 45 and BA 47). Temporal lobe endpoints were distributed across the inferior temporal cortex with a very high density of endpoints in the temporal pole.

3.2.1. The ILF and IFOF

The peri-VWFA fascicular network includes three major fiber tracts. Two of these are large and well-known. The inferior fronto-occipito fasciculus (IFOF) contains fibers passing from much of the occipital lobe, including VOT cortex, through the external capsule to inferior frontal cortex. The inferior longitudinal fasciculus (ILF) connects much of the occipital lobe, including VOT cortex, to the anterior and medial temporal lobe. While the ILF and IFOF are major fascicles, their endpoints are not specific to the VWFA. For some subjects the ILF and IFOF did not contain endpoints in the functionally defined VWFA voxels; rather, the fascicles simply passed nearby, but it is likely that smaller fiber bundles from the VWFA enter these major tracts. To identify such bundles confidently will require more sensitive diffusion analysis techniques than we have implemented here.

3.2.2. The vertical occipital fasciculus

A third fiber group appears consistently near the VWFA in each subject. This tract ascends from the OTS, immediately lateral to ILF fibers, before branching laterally toward its cortical endpoints in the lateral occipital and inferior parietal lobes. The tract appears

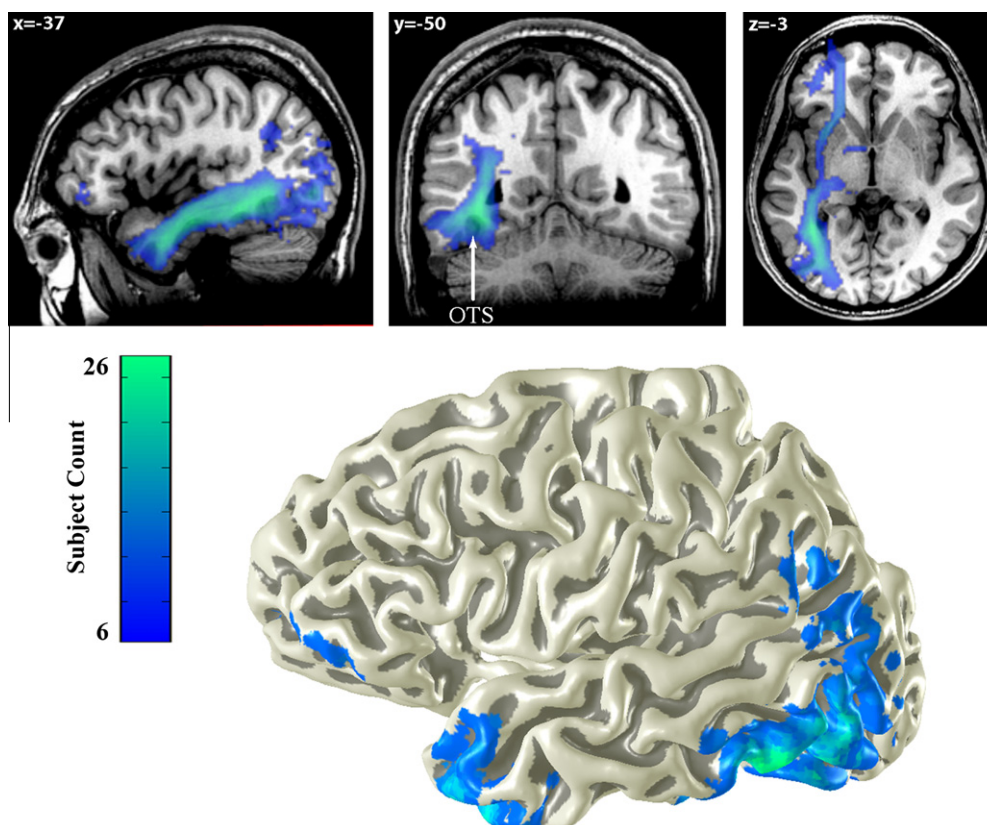


Fig. 4. Average white matter tracts connecting to the VWFA. The top panel shows a heat-map of the number of subjects ($N = 27$) with VWFA white matter connections passing through each voxel. Three distinct fiber tracts are consistently identified across subjects: The inferior longitudinal fasciculus (ILF, see sagittal slice), the vertical occipital fasciculus (VOF, see coronal slice) and the inferior frontal occipital fasciculus (IFOF, see axial slice). The location of the occipital temporal sulcus (OTS) is marked on the coronal plane. The bottom panel shows the cortical endpoints of these tracts displayed on a 3-dimensional rendering of a subject's cortical surface.

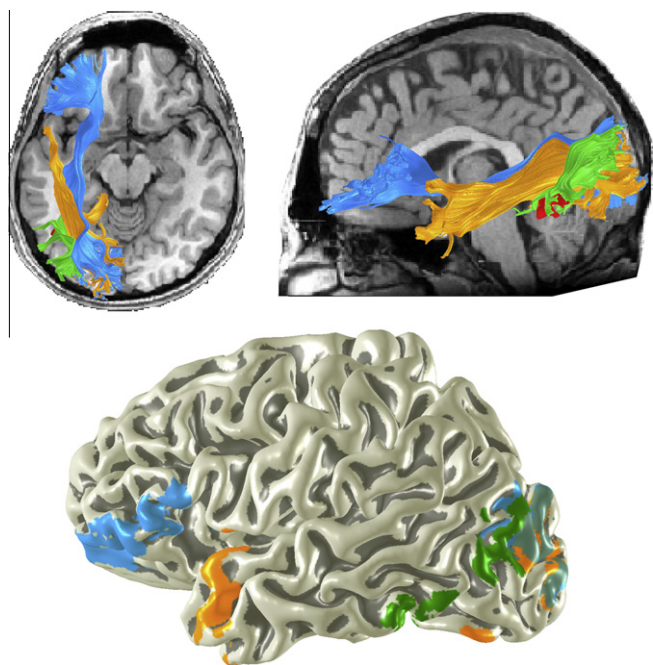


Fig. 5. Major white matter tracts passing near the VWFA. The ILF (orange) and the IFOF (blue) are large fascicles connecting much of the occipital lobe including ventral occipital temporal (VOT) cortex to anterior brain regions. The vertical occipital fasciculus (green) connects the occipitotemporal sulcus (and other VOT regions) including voxels identified as the VWFA to the lateral portion of the occipital parietal junction. The tracts are shown for a single representative subject. The bottom panel shows the endpoints of these three tracts on a 3-D rendering of the same subject's cortical surface.

to connect VOT cortex to the lateral occipital parietal junction, including the posterior angular gyrus and lateral superior occipital lobe. The fiber group's ventral terminations are consistently within or near the functionally defined VWFA voxels.

This fiber group is the vertical occipital fasciculus (VOF) of Wernicke. It was a major theoretical focus in earlier work on acquired alexia by Greenblatt (Greenblatt, 1973). A homologous tract has been identified in the macaque monkey based on autoradiographic tracers (Schmahmann & Pandya, 2006). The VOF can be identified on individual subjects' fiber orientation maps using simple methods described in the Supplemental materials (Supplemental Fig. S1A).

As with most fiber tracts, there is some between-subject variation in the trajectory and VOF endpoints. The variation of the VOF we have found is illustrated in data from three subjects, (Supplemental Fig. S1B). The estimated VOF connects to different portions of the functionally identified VWFA within ventral occipital cortex. The dorsal endpoints of the VOF connect regions in the lateral occipital lobe, inferior parietal lobe, or both.

3.3. Visualizations of the VWFA's neighborhood

3.3.1. Peri-VWFA streamlines

The three principal peri-VWFA fiber groups and their endpoints can be estimated in individual subjects. The rendering in Fig. 5 shows these groups and their terminations on the cortical surface. The same pattern is observed in all of the individuals in our data set; the precise location and endpoints of the tracts varies with respect to gyral landmarks, but the gross anatomy of these pathways is largely consistent between individuals. These diffusion estimates show the major organization; more refined analyses will be required to obtain rigorous estimates at the millimeter scale.

3.3.2. A slice of the VWFA neighborhood

The proximity of the VWFA to retinotopically defined visual field maps is particularly clear when visualized in volume space. In almost every subject the VWFA abuts VO-1 and VO-2 and is near hV4, TO-1, and TO-2 (Wandell, 2011; Wandell et al., 2012). Fig. 6 shows axial slices and Supplemental Fig. S2 shows coronal slices near the VWFA. These images denote the major white matter projections and the nearby visual field maps in the left hemisphere. The images are from a typical subject.

In this subject the VWFA abuts the VO-1/VO-2 field maps as well as the TO-1/TO-2 field maps. Our understanding of the specific function of the VO maps is very incomplete, but they appear to have a role in the perception of form and color (Meadows, 1974a, 1974b; Zeki, 1990). Most of the surface area within these maps is driven by signals from the central retina, the temporal dynamics in this region is sluggish, and the region responds well to all three dimensions of color. The TO maps are almost certainly involved in the perception of visual motion (Salzman, Britten, & Newsome, 1990; Tootell et al., 1995; Zeki, 1980) and they are highly responsive to manipulations of attention (Beauchamp, Cox, & Deyoe, 1997; Gandhi, Heeger, & Boynton, 1999; O'Craven, Rosen, Kwong, Treisman, & Savoy, 1997). This part of cortex is likely to carry important information about eye movement control that is important for reading (Komatsu & Wurtz, 1988a, 1988b; Newsome, Wurtz, & Komatsu, 1988).

Ventral occipital cortex near the VWFA is frequently labeled as the fusiform face area (FFA). There are several distinct face-responsive regions near the VWFA (Weiner & Grill-Spector, 2010).

The arrangement near the VWFA for another subject is shown Supplemental Fig. S3. In that subject, the VWFA abuts VO-1/VO-2 and is spatially separated from the TO-1/TO-2 maps. The relative position of each functional module maintains a relatively consistent layout with respect to these maps and white matter fascicles. The word-selective voxels always fall medial and inferior to TO-1/TO-2 and lateral to VO-1/VO-2. However the cortical surface area occupied by word-selective VWFA voxels varies between subjects.

4. Discussion

The VWFA is located near ventral visual field maps and probably receives direct input from these maps (Fig. 1). The VWFA is adjacent and lateral to visual field maps VO-1 and VO-2 in all subjects. Between subjects, the VWFA position varies significantly with respect to sulcal and gyral landmarks and less with respect to the visual field maps. Within subjects the responses that define the VWFA position are relatively stable across time (Fig. 2).

The ILF and IFOF pass within close proximity of the VWFA and are likely to contain axon bundles with significant information for seeing words. The vertical occipital fasciculus of Wernicke connects regions within VOT, and likely within the VWFA, to the lateral occipital parietal junction and the posterior angular gyrus (Figs. 4 and 5).

4.1. Circuits in visual cortex for seeing words

Visual information, including the information about words on a page, first enters cortex in primary visual cortex (V1). V1 is dominated by neurons that have a small field of view (receptive field) compared to neurons in other visual field maps. Responses of V1 neurons can be modeled with simple models (Cavanaugh, Bair, & Movshon, 2002; Heeger, Simoncelli, & Movshon, 1996; Kay, Naselaris, Prenger, & Gallant, 2008). As one measures the response along the anterior field maps, the receptive field size of individual neurons within the primate cortex increases (Van Essen, Newsome, & Maunsell, 1984). The increasing field of view has been confirmed in human fMRI measurements of the receptive field of voxels –

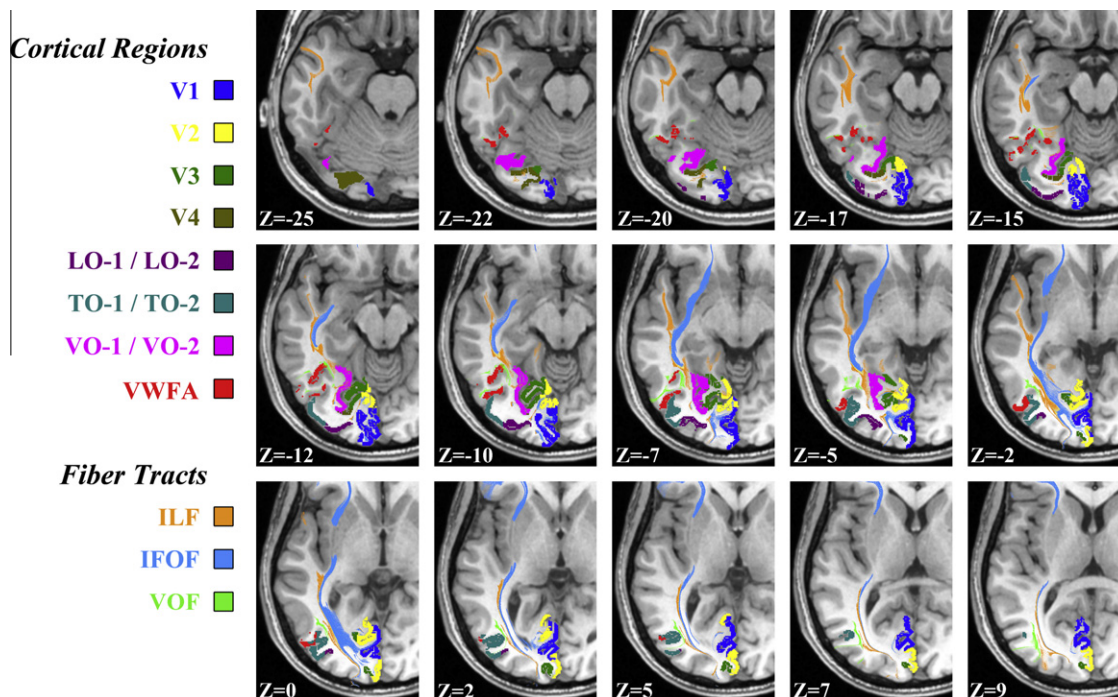


Fig. 6. Axial slices showing the VWFA, nearby white matter fascicles, and visual field maps. The visual word form area (VWFA) is shown in red. For this individual, cortical voxels were identified corresponding to the following field maps: V1, V2, V3, V4, lateral-occipital 1 and 2 (LO-1/LO-2), temporal-occipital 1 and 2, (TO-1/TO-2), ventral-occipital 1 and 2 (VO-1/VO-2). White matter voxels in peri-VWFA white matter fascicles were identified from diffusion-weighted images: inferior longitudinal fasciculus (ILF), inferior frontal occipital fasciculus (IFOF), and the vertical occipital fasciculus (VOF).

which is called the population receptive field (pRF, Dumoulin & Wandell, 2008). The pRF size increase in maps near the VWFA. A VO-1 pRF is about fivefold compared to V1 pRF size (Kay, Winawer, Mezer, & Wandell, submitted for publication). The difference in pRF size from V1 to the VWFA is a gradual change, rather than an abrupt loss of position sensitivity, and even the latest stages of visual processing likely retain some position sensitivity (Rauschecker et al., 2011).

Most contrast patterns evoke a response in V1 and V2, but voxels in the ventral occipital and lateral occipital maps appear to favor spatial patterns that distinguish between the statistical properties of different shapes – such as faces, objects and orthography. Hence, from V1 to VOT cortex the neuronal field of view widens and the neuronal pattern sensitivity narrows. Furthermore, the stimuli that evoke a response from voxels in these maps are not coupled uniquely in any obvious way to parameters of the image spatial contrast. Rather, circuitry in the visual field maps appears to transform many types of spatial features into an abstract shape representation (Grill-Spector, Kushnir, Edelman, Itzchak, & Malach, 1998; Rauschecker et al., 2011), and the properties of the shape representation determine the response efficacy in the VWFA and nearby visual field maps. Multiple circuits within visual cortex may contribute to the computation of the shape representation. For example, the VWFA is located near both the VO and TO maps, and it responds to shape information abstracted either from conventional line contrast or shapes defined by coherent dot motion, suggesting that both the VO and TO maps can provide input to the VWFA (Rauschecker et al., 2011).

4.2. Is the VWFA reading circuitry?

The question as to whether the VWFA is used while reading seems largely settled: VWFA circuitry is responsive to visual word forms (Dehaene et al., 2002; Salmelin et al., 1996, 2000; Wandell, 2011; Wandell et al., 2012); damage to the VWFA or nearby white matter produces reading deficits (Epelbaum et al., 2008; Gaillard

et al., 2006; Greenblatt, 1973, 1976; Iragui & Kritchevsky, 1991) VWFA responses are weak in poor readers (Maisog et al., 2008; Wandell et al., 2012) during development reading performance improvements are correlated with increases in VOT responses to written words (Ben-Shachar et al., 2011).

Like cortex in general, VWFA circuitry is probably used to support multiple tasks (Ben-Shachar, Dougherty, Wandell, et al., 2007). Some propose to adjudicate whether the VWFA is “predominantly used in reading” or “a more general visual processor used in reading but also in other visual tasks (Vogel et al., 2011, abstract).” Whatever judgment is rendered about the balance, it is clear that V1 communicates orthography and other forms to the rest of visual cortex; similarly, the VWFA communicates orthographic signals to other parts of cortex. The VWFA contributes essential information to the reading network.

Analyses of reading circuitry will eventually be supported by computational models of the transformation from visual input to word shape and eventually to meaning. The precise contribution of the VWFA compared to other circuits awaits such modeling.

4.3. Does the VWFA have a privileged role in VOT reading circuitry?

Anterior ventral temporal lobe locations may also be important for reading (Nobre et al., 1994). Currently, there are significant technical challenges that severely limit fMRI measurements in these areas anterior to the VWFA (Winawer et al., 2010). While an essential component of the reading circuitry, the VWFA does not act in isolation: the visual field maps are important inputs to the VWFA, and the precise VWFA outputs are known only approximately.

We report for the first time that the vertical occipital fasciculus of Wernicke terminates in both the VWFA and the lateral occipital parietal junction including the angular gyrus. The diffusion estimates support Greenblatt’s discovery that lesions to this pathway cause pure alexia even when VOT cortex is spared (Greenblatt, 1973, 1976). Much prior work shows that lesions in white matter

pathways posterior to the VWFA, which are likely to deliver inputs from visual cortex, can also cause alexia (Binder & Mohr, 1992; Damasio & Damasio, 1983; Epelbaum et al., 2008). Hence, the VWFA appears to receive projections from visual cortex and it has access to a pathway that can carry signals forward to cortical language regions. The VWFA may have a privileged position in communicating information about words forms between visual and language areas (Devlin, Jamison, Gonnerman, & Matthews, 2006; Rauschecker et al., 2011). If all information about orthography passes through the VWFA, then disturbing the pathway between the VWFA and language areas would inevitably impair reading.

4.4. Reading and the single subject

Modern neuroimaging methods have adequate sensitivity to measure activity and structure in single subjects at millimeter resolution. Such methods are essential for understanding the neurological basis of phenomena in single subjects. Modern fMRI measures detect word-related responses in consistent locations in single subjects. Modern diffusion methods reliably identify major fascicles in individual subjects. Investigations based on data from single subjects offer better spatial resolution and have significant advantages over group methods when translating scientific findings into clinical practice.

Acknowledgments

This work was supported by NIH Grants EY015000 and EY03164 to Brian A. Wandell; an NSF Graduate Research Fellowship to Jason D. Yeatman; the Medical Scientist Training Program and a Bio-X Graduate Student Fellowship to Andreas Rauschecker. We thank Jonathan Winawer for help collecting retinotopy data and with definition of retinotopic maps. We thank Michal Ben-Shachar and Robert F. Dougherty for assistance with VWFA localizer data and diffusion weighted imaging data. We thank Lee M. Perry for help in collection and analyses of fMRI and diffusion data.

Appendix A. Supplementary material

Supplementary data associated with this article can be found, in the online version, at <http://dx.doi.org/10.1016/j.bandl.2012.04.010>.

References

- Amano, K., Wandell, B. A., & Dumoulin, S. O. (2009). Visual field maps, population receptive field sizes, and visual field coverage in the human MT+ complex. *Journal of Neurophysiology*, *102*(5), 2704–2718.
- Andrews, T. J., Halpern, S. D., & Purves, D. (1997). Correlated size variations in human visual cortex, lateral geniculate nucleus, and optic tract. *Journal of Neuroscience*, *17*(8), 2859–2868.
- Basser, P. J., Pajevic, S., Pierpaoli, C., Duda, J., & Aldroubi, A. (2000). In vivo fiber tractography using DT-MRI data. *Magnetic Resonance in Medicine*, *44*(4), 625–632.
- Beauchamp, M. S., Cox, R. W., & Deyoe, E. A. (1997). Graded effects of spatial and featural attention on human area MT and associated motion processing areas. *Journal of Neurophysiology*, *78*(1), 516–520.
- Ben-Shachar, M., Dougherty, R. F., Deutsch, G. K., & Wandell, B. A. (2007a). Contrast responsivity in MT+ correlates with phonological awareness and reading measures in children. *NeuroImage*, *37*(4), 1396–1406.
- Ben-Shachar, M., Dougherty, R. F., Deutsch, G. K., & Wandell, B. A. (2007b). Differential sensitivity to words and shapes in ventral occipito-temporal cortex. *Cerebral Cortex*, *17*(7), 1604–1611.
- Ben-Shachar, M., Dougherty, R. F., Deutsch, G. K., & Wandell, B. A. (2011). The development of cortical sensitivity to visual word forms. *Journal of Cognitive Neuroscience*, *23*(9), 2387–2399.
- Ben-Shachar, M., Dougherty, R. F., Wandell, B. A., Ben-Shachar, M., Dougherty, R. F., & Wandell, B. A. (2007). White matter pathways in reading. *Current Opinion in Neurobiology*, *17*(2), 258–270.
- Binder, J. R., & Mohr, J. P. (1992). The topography of callosal reading pathways. *Brain*, *115*, 1807–1826.
- Brem, S., Bach, S., Kucian, K., Guttorm, T. K., Martin, E., Lyytinen, H., et al. (2010). Brain sensitivity to print emerges when children learn letter-speech sound correspondences. *Proceedings of the National Academy of Sciences of the United States of America*, *107*(17), 7939–7944.
- Brewer, A. A., Liu, J., Wade, A. R., & Wandell, B. A. (2005). Visual field maps and stimulus selectivity in human ventral occipital cortex. *Nature Neuroscience*, *8*(8), 1102–1109.
- Cavanaugh, J. R., Bair, W., & Movshon, J. A. (2002). Nature and interaction of signals from the receptive field center and surround in macaque V1 neurons. *Journal of Neurophysiology*, *88*(5), 2530–2546.
- Chang, L. C., Jones, D. K., & Pierpaoli, C. (2005). Restore: Robust estimation of tensors by outlier rejection. *Magnetic Resonance in Medicine*, *53*(5), 1088–1095.
- Cohen, L., Lehericy, S., Chochon, F., Lemer, C., Rivaud, S., & Dehaene, S. (2002). Language-specific tuning of visual cortex? Functional properties of the visual word form area. *Brain*, *125*(Pt 5), 1054–1069.
- Cohen, L., Martinaud, O., Lemer, C., Lehericy, S., Samson, Y., Obadia, M., et al. (2003). Visual word recognition in the left and right hemispheres: Anatomical and functional correlates of peripheral alexias. *Cerebral Cortex*, *13*(12), 1313–1333.
- Damasio, A. R., & Damasio, H. (1983). The anatomic basis of pure alexia. *Neurology*, *33*(12), 1573–1583.
- Dehaene, S., & Cohen, L. (2011). The unique role of the visual word form area in reading. *Trends in Cognitive Sciences*, *15*(6), 254–262.
- Dehaene, S., Le Clec, H. G., Poline, J. B., Le Bihan, D., & Cohen, L. (2002). The visual word form area: A prelexical representation of visual words in the fusiform gyrus. *NeuroReport*, *13*(3), 321–325.
- Dehaene, S., Pegado, F., Braga, L. W., Ventura, P., Nunes Filho, G., Jobert, A., et al. (2011). How learning to read changes the cortical networks for vision and language. *Science*, *330*(6009), 1359–1364.
- Devlin, J. T., Jamison, H. L., Gonnerman, L. M., & Matthews, P. M. (2006). The role of the posterior fusiform gyrus in reading. *Journal of Cognitive Neuroscience*, *18*(6), 911–922.
- Dougherty, R. F., Koch, V. M., Brewer, A. A., Fischer, B., Modersitzki, J., & Wandell, B. A. (2003). Visual field representations and locations of visual areas V1/2/3 in human visual cortex. *Journal of Vision*, *3*(10), 586–598.
- Dumoulin, S. O., & Wandell, B. A. (2008). Population receptive field estimates in human visual cortex. *NeuroImage*, *39*(2), 647–660.
- Epelbaum, S., Pinel, P., Gaillard, R., Delmaire, C., Perrin, M., Dupont, S., et al. (2008). Pure alexia as a disconnection syndrome: New diffusion imaging evidence for an old concept. *Cortex*, *44*(8), 962–974.
- Friston, K. J., & Ashburner, J. (2004). Generative and recognition models for neuroanatomy. *NeuroImage*, *23*(1), 21–24.
- Gaillard, R., Naccache, L., Pinel, P., Cleemenceau, S., Volle, E., Hasboun, D., et al. (2006). Direct intracranial fMRI and lesion evidence for the causal role of left inferotemporal cortex in reading. *Neuron*, *50*(2), 191–204.
- Gandhi, S. P., Heeger, D. J., & Boynton, G. M. (1999). Spatial attention affects brain activity in human primary visual cortex. *Proceedings of the National Academy of Sciences of the United States of America*, *96*(6), 3314–3319.
- Glover, G. H. (1999). Simple analytic spiral k-space algorithm. *Magnetic Resonance in Medicine*, *42*(2), 412–415.
- Greenblatt, S. H. (1973). Alexia without agraphia or hemianopsia. Anatomical analysis of an autopsied case. *Brain*, *96*(2), 307–316.
- Greenblatt, S. H. (1976). Subangular alexia without agraphia or hemianopsia. *Brain and Language*, *3*(2), 229–245.
- Grill-Spector, K., Kushnir, T., Edelman, S., Itzhak, Y., & Malach, R. (1998). Cue-invariant activation in object-related areas of the human occipital lobe. *Neuron*, *21*(1), 191–202.
- Heeger, D. J., Simoncelli, E. P., & Movshon, J. A. (1996). Computational models of cortical visual processing. *Proceedings of the National Academy of Sciences of the United States of America*, *93*, 623–627.
- Iragui, V. J., & Krichevsky, M. (1991). Alexia without agraphia or hemianopsia in parietal infarction. *Journal of Neurology, Neurosurgery and Psychiatry*, *54*(9), 841–842.
- Kay, K., Winawer, J., Mezer, A., & Wandell, B. A. (submitted for publication). The emergence of position and size tolerance in human visual cortex.
- Kay, K. N., Naselaris, T., Prenger, R. J., & Gallant, J. L. (2008). Identifying natural images from human brain activity. *Nature*, *452*(7185), 352–355.
- Kinsbourne, M., & Warrington, E. K. (1963). The localizing significance of limited simultaneous visual form perception. *Brain*, *86*, 697–702.
- Komatsu, H., & Wurtz, R. H. (1988a). Relation of cortical areas MT and MST to pursuit eye movements. I. Localization and visual properties of neurons. *Journal of Neurophysiology*, *60*(2), 580–603.
- Komatsu, H., & Wurtz, R. H. (1988b). Relation of cortical areas MT and MST to pursuit eye movements. III. Interaction with full-field visual stimulation. *Journal of Neurophysiology*, *60*(2), 621–644.
- Maisog, J. M., Einbinder, E. R., Flowers, D. L., Turkeltaub, P. E., & Eden, G. F. (2008). A meta-analysis of functional neuroimaging studies of dyslexia. *Annals of the New York Academy of Sciences*, *1145*, 237–259.
- Maurer, U., Brem, S., Bucher, K., & Brandeis, D. (2005). Emerging neurophysiological specialization for letter strings. *Journal of Cognitive Neuroscience*, *17*(10), 1532–1552.
- Mccandliss, B. D., Cohen, L., & Dehaene, S. (2003). The visual word form area: Expertise for reading in the fusiform gyrus. *Trends in Cognitive Sciences*, *7*(7), 293–299.
- Meadows, J. (1974a). Disturbed perception of colours associated with localized cerebral lesions. *Brain*, *97*, 615–632.

- Meadows, J. (1974b). The anatomical basis of prosopagnosia. *Journal of Neurology, Neurosurgery And Psychiatry*, 37, 389–401.
- Mori, S., Crain, B. J., Chacko, V. P., & Van Zijl, P. C. (1999). Three-dimensional tracking of axonal projections in the brain by magnetic resonance imaging. *Annals of Neurology*, 45(2), 265–269.
- Newsome, W. T., Wurtz, R. H., & Komatsu, H. (1988). Relation of cortical areas MT and MST to pursuit eye movements. II. Differentiation of retinal from extraretinal inputs. *Journal of Neurophysiology*, 60(2), 604–620.
- Nobre, A. C., Allison, T., & McCarthy, G. (1994). Word recognition in the human inferior temporal lobe. *Nature*, 372(6503), 260–263.
- O'craven, K. M., Rosen, B. R., Kwong, K. K., Treisman, A., & Savoy, R. (1997). Voluntary attention modulates fMRI activity in human MT-MST. *Neuron*, 18(4), 591–598.
- Petersen, S. E., Fox, P. T., Snyder, A. Z., & Raichle, M. E. (1990). Activation of extrastriate and frontal cortical areas by visual words and word-like stimuli. *Science*, 249(4972), 1041–1044.
- Price, C. J., & Devlin, J. T. (2003). The myth of the visual word form area. *Neuroimage*, 19(3), 473–481.
- Price, C. J., & Devlin, J. T. (2011). The interactive account of ventral occipitotemporal contributions to reading. *Trends in Cognitive Sciences*, 15(6), 246–253.
- Price, C. J., Wise, R. J., Watson, J. D., Patterson, K., Howard, D., & Frackowiak, R. S. (1994). Brain activity during reading. The effects of exposure duration and task. *Brain*, 117(Pt 6), 1255–1269.
- Rauschecker, A. M., Bowen, R. F., Perry, L. M., Kevan, A. M., Dougherty, R. F., & Wandell, B. A. (2011). Visual feature-tolerance in the reading network. *Neuron*, 71(5), 941–953.
- Rohde, G. K., Barnett, A. S., Basser, P. J., Marengo, S., & Pierpaoli, C. (2004). Comprehensive approach for correction of motion and distortion in diffusion-weighted MRI. *Magnetic Resonance in Medicine*, 51(1), 103–114.
- Salmelin, R., Helenius, P., & Service, E. (2000). Neurophysiology of fluent and impaired reading: A magnetoencephalographic approach. *Journal of Clinical Neurophysiology*, 17(2), 163–174.
- Salmelin, R., Service, E., Kiesila, P., Uutela, K., & Salonen, O. (1996). Impaired visual word processing in dyslexia revealed with magnetoencephalography. *Annals of Neurology*, 40(2), 157–162.
- Salzman, C. D., Britten, K. H., & Newsome, W. T. (1990). Cortical microstimulation influences perceptual judgements of motion direction. *Nature*, 346(6280), 174–177.
- Schmahmann, J. D., & Pandya, D. N. (2006). *Fiber pathways of the brain*. New York: Oxford University Press.
- Tootell, R. B., Reppas, J. B., Kwong, K. K., Malach, R., Born, R. T., Brady, T. J., et al. (1995). Functional analysis of human MT and related visual cortical areas using magnetic resonance imaging. *Journal of Neuroscience*, 15(4), 3215–3230.
- Van Essen, D. C., Newsome, W. T., & Maunsell, J. H. (1984). The visual field representation in striate cortex of the macaque monkey: Asymmetries, anisotropies, and individual variability. *Vision Research*, 24(5), 429–448.
- Vogel, A. C., Miezin, F. M., Petersen, S. E., & Schlaggar, B. L. (2011). The putative visual word form area is functionally connected to the dorsal attention network. *Cerebral Cortex*.
- Wandell, B. A. (2011). The neurobiological basis of seeing words. *Annals of the New York Academy of Sciences*, 1224(1), 63–80.
- Wandell, B. A., Dumoulin, S. O., & Brewer, A. A. (2007). Visual field maps in human cortex. *Neuron*, 56(2), 366–383.
- Wandell, B. A., Rauschecker, A. M., & Yeatman, J. D. (2012). Learning to see words. *Annual Review of Psychology*, 63, 31–53.
- Wandell, B. A., & Winawer, J. (2010). Imaging retinotopic maps in the human brain. *Vision Research*.
- Warrington, E. K., & Shallice, T. (1980). Word-form dyslexia. *Brain*, 103(1), 99–112.
- Weiner, K. S., & Grill-Spector, K. (2010). Sparsely-distributed organization of face and limb activations in human ventral temporal cortex. *Neuroimage*, 52(4), 1559–1573.
- Winawer, J., Horiguchi, H., Sayres, R. A., Amano, K., & Wandell, B. A. (2010). Mapping hV4 and ventral occipital cortex: The venous eclipse. *Journal of Vision*, 10(5), 1.
- Yeatman, J. D., Dougherty, R. F., Rykhlevskaia, E., Sherbondy, A. J., Deutsch, G. K., Wandell, B. A., et al. (2011). *Anatomical properties of the arcuate fasciculus predict phonological and reading skills in children*. *Journal of Cognitive Neuroscience*.
- Zeki, S. (1980). The response properties of cells in the middle temporal area (area MT) of owl monkey visual cortex. *Proceedings of the Royal Society of London. Series B: Biological Sciences*, 207(1167), 239–248.
- Zeki, S. (1990). A century of cerebral achromatopsia. *Brain*, 113, 1721–1777.